A Reaction Engineering Approach to the Problem of Concrete Carbonation

Steel bars in reinforced concrete are protected from corrosion by the high pH environment of the surrounding concrete. This alkaline environment is destroyed by the reaction of atmospheric CO_2 with the $Ca(OH)_2$ of the concrete mass. When this process, called carbonation of concrete, reaches the reinforcing bars, corrosion of the latter may commence. In this paper, the physiochemical processes in this phenomenon are presented and modeled mathematically. The mathematical model is fairly complex, but certain simplifying assumptions are possible, which lead to the formation of a "carbonation front" and to a simple analytical expression for the evolution in time of this front, in terms of the composition parameters of cement and concrete and of the environmental conditions. This simple expression is in very good agreement with experimental results obtained in this and in previous studies. The effect of some parameters on the carbonation front propagation is also discussed.

V. G. Papadakis
C. G. Vayenas
Institute of Chemical Engineering and
High Temperature Chemical Processes
Department of Chemical Engineering

M. N. Fardis
Department of Civil Engineering
University of Patras
GR-26110 Patras, Greece

Introduction

Concrete is the most widely used construction material. Its success can be attributed not only to its low cost but also to its long record of satisfactory performance in service. This good performance includes its durability, which is much superior to that of its main competitors, steel and timber. In the last two decades, however, the instances of unsatisfactory durability of concrete structures have increased at an alarming rate, particularly in the most developed parts of the world.

The most common durability problem is corrosion of the reinforcing steel in reinforced concrete. Corrosion reduces the available cross-sectional area of a reinforcing bar and hence its strength, and introduces a bursting internal pressure on the concrete surrounding the bar, since the volume of the corrosion products exceeds by far that of the corroding metal. This causes spalling of the concrete covering the reinforcement and splitting concrete cracks parallel to the bar. Consequently, the connection between the reinforcement and the concrete is almost lost, and the contribution of the former to the strength is drastically reduced. Very often the safety and appearance problems caused by reinforcement corrosion before the end of the structure's useful lifetime are so severe that the structure either has to be demolished or requires very costly general repair and strengthening.

In response to this serious problem, the engineering community has staged in recent years a significant research effort, aiming at developing a deeper understanding of the mechanisms leading to reinforcement corrosion as well as effective measures to control it. In concrete, reinforcing bars are protected from corrosion by a thin oxide layer which is formed and maintained on their surface due to the highly alkaline environment of the surrounding concrete (pH values around 13). The alkalinity of the concrete mass is due to the $Ca(OH)_2$ produced during the reaction of the constituents of cement with water which causes the hardening and the development of strength of cement and concrete (Brunauer and Copeland, 1964). Depassivation of reinforcing bars occurs either when chloride ions diffuse in the pore water and reach the bars or when the pH value of the concrete surrounding the bar drops below 9, due to the diffusion of atmospheric CO_2 and its reaction with the $Ca(OH)_2$ of the concrete mass, or by a combination of these two mechanisms, in which the second mechanism accelerates the first. The former mechanism predominates in marine environments, in coastal areas, and when deicing salts come in contact with the concrete surface (pavements and bridge decks, floors of parking garages, etc.). The second mechanism, commonly called "carbonation of concrete," is predominant in all other cases, especially in urban environments with high concentration of CO_2 in the atmosphere.

Pereira and Hegedus (1984) were the first to recognize that concrete reinforcement depassivation by chloride ions can be treated as a classical reaction engineering problem. They developed a quantitative chloride ion diffusion-reaction model which

Correspondence concerning this paper should be addressed to C. G. Vayenas.

was found to be in very good agreement with experiment. The literature is also rich in studies of concrete carbonation, aiming at developing empirical or semiempirical relations for the prediction of the rate of carbonation, and hence of the time required for depassivation of the reinforcing steel (e.g., Hamada, 1969; Schiessl, 1976; Tuutti, 1982; Nagataki et al., 1986; Richardson, 1988).

In the present paper, the physicochemical processes involved in concrete carbonation are discussed and modeled mathematically, using basic principles and methods of reaction engineering. Thus, a fundamental model is developed for the prediction of the rate of concrete carbonation, in terms of the pertinent material parameters (composition of cement and concrete, porosity and pore size distribution, etc.) and of the environmental conditions (CO_2 concentration relative, humidity and temperature). For the usual range of the values of these parameters, the model predicts the formation of a "carbonation front," separating fully-carbonated areas from those in which CO_2 diffusion has not started yet. A simple analytical expression is derived for the rate of propagation of the carbonation front. The model is validated by comparing its predictions with experimental results obtained in this and previous studies, in environments of normal or high concentrations of CO_2. The model can be used to study the effect of various parameters on the rate of carbonation and to develop rules and specifications for the control of some of these parameters so that the rate of carbonation is reduced to acceptable levels.

Physicochemical Considerations

The carbonation of concrete is a complex physicochemical process. The process takes place in the cement paste component of concrete, whereas aggregates, which constitute the major part of the mass and volume of concrete, are essentially an inert filler, at least as far as carbonation is concerned. However, since the presence of aggregates affects certain important parameters, such as the effective diffusivity of CO_2, all quantities used in the model refer to the total mass of concrete.

The process of carbonation involves gaseous, dissolved and solid reactants. The solids which react with CO_2 include not only $Ca(OH)_2$, but also the main strength element of cement paste: $3CaO \cdot 2SiO_2 \cdot 3H_2O$ (CSH = calcium silicate hydrate); unhydrated constituents, $3CaO \cdot SiO_2$ (C_3S = tricalcium silicate) and $2CaO \cdot SiO_2$ (C_2S = dicalcium silicate). Calcium silicate hydrate is the product of the gradual hydration of these two basic components of Portland cement: C_3S and C_2S. These two hydration reactions also lead to formation of $Ca(OH)_2$. Consequently, in order to model the process of carbonation, one must also take into account the hydration process, since the latter is the main source of $Ca(OH)_2$ formation and its other reactants (C_3S, C_2S) and products (CSH) are also susceptible to reaction with CO_2.

Hydration reactions

The chemistry of hydration of Portland cement has been reviewed thoroughly (e.g., Brunauer and Copeland, 1964; Bensted, 1983; Frigione, 1983; Taylor, 1986). There are two major hydration reactions leading to the formation of CSH:

$$2(3CaO \cdot SiO_2) + 6H_2O \xrightarrow{r_{H,C_3S}} (3CaO \cdot 2SiO_2 \cdot 3H_2O) + 3Ca(OH)_2 \quad (1)$$

$$2(2CaO \cdot SiO_2) + 4H_2O \xrightarrow{r_{H,C_2S}} (3CaO \cdot 2SiO_2 \cdot 3H_2O) + Ca(OH)_2 \quad (2)$$

The rate of CSH formation, $r_{H,CSH}$, is then given by:

$$r_{H,CSH} = (1/2)(r_{H,C_3S} + r_{H,C_2S}) \quad (3)$$

Parallel hydration reactions lead to the consumption of $4CaO \cdot Al_2O_3 \cdot Fe_2O_3$ (C_4AF = calcium aluminoferrite) and $3CaO \cdot Al_2O_3$ (C_3A = tricalcium aluminate):

$$(4CaO \cdot Al_2O_3 \cdot Fe_2O_3) + 2Ca(OH)_2 + 2(CaSO_4 \cdot 2H_2O) + 18H_2O \xrightarrow{r_{H,C_4AF,\bar{S}}} (6CaO \cdot Al_2O_3 \cdot Fe_2O_3 \cdot 2CaSO_4 \cdot 24H_2O) \quad (4a)$$

$$(3CaO \cdot Al_2O_3) + CaSO_4 \cdot 2H_2O + 10H_2O \xrightarrow{r_{H,C_3A,\bar{S}}} (3CaO \cdot Al_2O_3 \cdot CaSO_4 \cdot 12H_2O) \quad (4b)$$

$$(4CaO \cdot Al_2O_3 \cdot Fe_2O_3) + 4Ca(OH)_2 + 22H_2O \xrightarrow{r_{H,C_4AF}} (6CaO \cdot Al_2O_3 \cdot Fe_2O_3 \cdot 2Ca(OH)_2 \cdot 24H_2O) \quad (5a)$$

$$(3CaO \cdot Al_2O_3) + Ca(OH)_2 + 12H_2O \xrightarrow{r_{H,C_3A}} (3CaO \cdot Al_2O_3 \cdot Ca(OH)_2 \cdot 12H_2O) \quad (5b)$$

Reactions 4a and 4b dominate in the presence of gypsum, which is always present in Portland cement. Reaction 4b, which consumes most of the gypsum, proceeds via intermediate formation of ettringite ($3CaO \cdot Al_2O_3 \cdot 3CaSO_4 \cdot 32H_2O$) which plays an important role in preventing "flash setting" in concrete (Bensted, 1983; Frigione, 1983; Taylor, 1986). Reactions 5a and 5b dominate when practically all the gypsum has been consumed.

Solid $Ca(OH)_2$ is formed by reactions 1 and 2 and consumed by reactions 4a, 5a and 5b. Consequently, the rate of $Ca(OH)_2$ formation from the hydration reactions, $r_{H,CH}$, can be expressed as:

$$r_{H,CH} = (3/2)r_{H,C_3S} + (1/2)r_{H,C_2S} - 2r_{H,C_4AF,\bar{S}} - 4r_{H,C_4AF} - r_{H,C_3A} \quad (6)$$

The kinetics of reactions 1, 2, 5a and 5b have been presented by Brunauer and Copeland (1964). Interestingly, the presence of gypsum has been reported to have only a small effect on the rates of hydration of C_4AF and C_3A (Frigione, 1983). We have found that the experimentally observed kinetic behavior, which is in good agreement with more recent work (Taylor, 1986), can be approximated well by the power law kinetic expressions given in Table 1. These expressions hold for ordinary Portland cement (OPC) of normal fineness (so-called Type-I cement). As shown in Figure 1, the agreement between experiment and these pow-

Table 1. Power-Law Kinetic Expressions Used to Approximate the Hydration of Ordinary Portland Cement

Hydration rate of constituent i:

$$r_{H,i} = (k_{H,i}/[i]_0^{n_i-1})[i]^{n_i}$$

Hydrated fraction of constituent i:

$$F_i = 1 - [i]/[i]_0 = 1 - (1 - k_{H,i}(t_{cu} + t)(1 - n_i))^{1/(1-n_i)}$$

Constituent i	C_3S	C_2S	C_3A	C_4AF
n_i	2.65	3.10	2.41	3.81
$k_{H,i}(20°C) \times 10^5$ (s^{-1})	1.17	0.16	2.46	1.00

er-law kinetics is quite satisfactory. It is worth noting that the characteristic time constants of these reactions is of the order of 20 days.

Tricalcium silicate (C_3S) and dicalcium silicate (C_2S) constitute more than 80 mol % of the mass of Portland cement and, consequently, the last three terms in Eq. 6 can, to a first approximation, be neglected in most applications. These terms, however, can become important and cause an acceleration in the process of carbonation when certain additives (e.g., fly ash) are blended with ordinary Portland cement.

It is worth mentioning that in practice, during the first few days after mixing and pouring of the concrete, care is taken to maintain the pores of the young concrete filled with water so that the hydration reactions, Eqs. 1, 2, 4 and 5, can proceed in excess H_2O. This process, called "curing," lasts in practice for a time t_{cu} of about 7 days, after which evaporation of water from the concrete surface is allowed and equilibration in the chemical potential of H_2O is gradually established between the external environment and the concrete mass. Since concrete pores are filled entirely with water during the curing period t_{cu}, carbonation practically does not take place during this period. Consequently, throughout this paper, initial conditions ($t = 0$) refer to the end of the curing period t_{cu}. The expressions given in Table 1 can be used to compute the initial ($t = 0$) concentrations of the

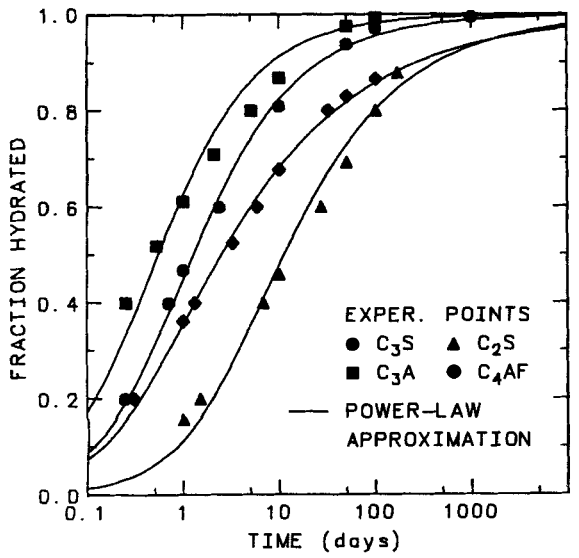

Figure 1. Hydration speed of the major constituents of ordinary Portland cement.

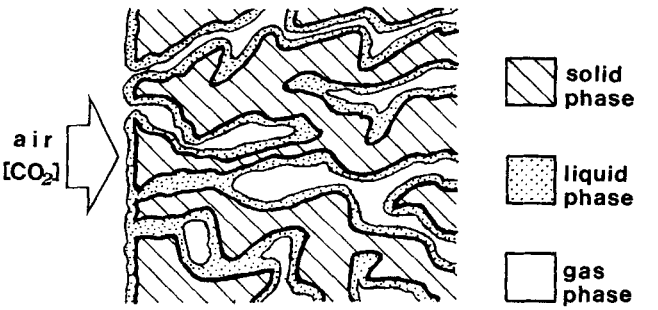

Figure 2. CO_2(g) diffusion in concrete pores.

constituents of concrete in terms of their values at the beginning of the curing period ($t_{cu} = 0$). The subscript "0" is used throughout the paper to denote the beginning of the curing period, $t_{cu} = 0$.

Carbonation of $Ca(OH)_2$

Water is always present in larger or lesser amounts in the pores of hardened cement paste and plays a key role in the process of carbonation. The role of water is twofold: first, it blocks the pores and thus hinders diffusion of CO_2 through the pores; second, it provides a medium for reaction between CO_2 and $Ca(OH)_2$.

The above qualitative considerations can explain why the rate of carbonation has been reported to go through a maximum with increasing ambient relative humidity (Schiessl, 1976). At very low ambient relative humidity levels, CO_2 can diffuse fast, but most pores are dry and the rate of carbonation is very slow. At high ambient relative humidity levels, practically all the pores are filled with water, therefore diffusion of CO_2 becomes very slow.

The overall reaction between $Ca(OH)_2$(s) and CO_2(g),

$$Ca(OH)_2(s) + CO_2(g) \rightarrow CaCO_3(s) + H_2O \qquad (7)$$

consists of several elementary steps which take place in the aqueous film on the pore walls (Figure 2). One can distinguish the $Ca(OH)_2$ dissolution step:

$$Ca(OH)_2(s) \overset{r_D}{\rightleftharpoons} Ca^{2+}(aq) + 2OH^-(aq) \qquad (8)$$

and the other elementary steps which constitute the overall reaction:

$$Ca^{2+}(aq) + 2OH^-(aq) + CO_2(g) \xrightarrow{r_{CH}} CaCO_3(s) + H_2O \qquad (9)$$

These are

$$CO_2(g) \xrightarrow{r_{CH}} CO_2(aq) \qquad (9a)$$

$$CO_2(aq) + OH^-(aq) \xrightarrow{r_{CH}} HCO_3^-(aq) \qquad (9b)$$

$$HCO_3^-(aq) + OH^-(aq) \xrightarrow{r_{CH}} CO_3^{2-}(aq) + H_2O \quad (9c)$$

$$Ca^{2+}(aq) + CO_3^{2-}(aq) \xrightarrow{r_{CH}} CaCO_3(s) \quad (9d)$$

The kinetics of reaction 9 and of the elementary steps (Eqs. 9a–9d) have been studied in detail (Dankwerts, 1970). It has been found that the rate expression

$$r_{CH} = HRTk_2[OH^-]_{eq}[CO_2] \quad (10)$$

provides a good approximation for pH values above ten. In the above expression, H is Henry's constant for CO_2 dissolution in H_2O, k_2 is the rate constant between CO_2 and OH^- ions, $[OH^-]_{eq}$ is the OH^- concentration in a saturated $Ca(OH)_2$ solution, and $[CO_2]$ is the molar concentration in the gas phase.

It should be noted that the diffusivity of OH^- and therefore of $Ca(OH)_2(aq)$, which we will use from now on to denote $Ca^{2+}(aq) + 2OH^-(aq)$, is typically of the order of 10^{-9} m^2/s in aqueous solutions. Consequently, $Ca(OH)_2(aq)$ is able to diffuse at a finite rate normal to the outer surface of porous concrete and therefore the local rate of $Ca(OH)_2(s)$ dissolution, r_D, may differ from the local rate of $Ca(OH)_2(aq)$ consumption, r_{CH}, as $Ca(OH)_2(aq)$ will tend to migrate from higher to lower pH regions. The rate of $Ca(OH)_2(s)$ dissolution can be approximated well by (Ramachandran and Sarma, 1969):

$$r_D = (1/2)\epsilon f_w k_s a_{s,CH}([OH^-]_{eq} - [OH^-]) \quad (11)$$

In the above expression, ϵ is concrete porosity, f_w is volume fraction of pores occupied by the aqueous film, k_s is the mass transfer coefficient for the dissolution of $Ca(OH)_2(s)$, $a_{s,CH}$ is the exposed surface area of $Ca(OH)_2(s)$ per unit volume of concrete, and $[OH^-]$ is the local concentration of OH^- in the liquid phase of pores.

Carbonation of CSH and unhydrated components

All the principal reactants and products of the hydration reactions of Portland cement are susceptible to carbonation in the presence of moisture. The ultimate carbonation products are normally alumina gel, calcite, iron oxide gel, and silica gel. The main reactions are:

$$(3CaO \cdot 2SiO_2 \cdot 3H_2O) + 3CO_2 \xrightarrow{r_{CSH}} (3CaCO_3 \cdot 2SiO_2 \cdot 3H_2O) \quad (12)$$

$$(3CaO \cdot SiO_2) + 3CO_2 + vH_2O \xrightarrow{r_{C_3S}} SiO_2 \cdot vH_2O + 3CaCO_3 \quad (13)$$

$$(2CaO \cdot SiO_2) + 2CO_2 + vH_2O \xrightarrow{r_{C_2S}} SiO_2 \cdot vH_2O + 2CaCO_3 \quad (14)$$

There is strong evidence that for the other hydrated and unhydrated constituents of hardened cement paste, carbonation is limited to a surface zone with the bulk of the crystallites remaining unaffected (Bensted, 1983). Consequently, carbonation of these components needs not to be included in the model. The main products of carbonation are $CaCO_3$ originating from $Ca(OH)_2(s)$ and $(3CaCO_3 \cdot 2SiO_2 \cdot 3H_2O)$ originating from CSH according to reaction 12. There have been only qualitative studies of the kinetics of reactions 12–14 (Sauman, 1971; Baird et al., 1975; Goodbrake et al., 1979; Suzuki et al., 1985) which can be reasonably assumed to be first order in $[CO_2]$ and in the exposed surface areas $\alpha_{s,CSH}$, α_{s,C_3S} and α_{s,C_2S} of the solids CSH, C_3S and C_2S, respectively. To a first approximation, one can compute these surface areas in concrete by multiplying the total surface area with the solid mole fraction of each of these constituents in the concrete. These previous studies, which indicate that, for $p_{CO_2} = 1$ bar, carbonation of these components is almost complete in less than 48 h, can serve to establish a lower limit for the values of the kinetic constants of reactions 12–14. Fortunately, the model predictions are insensitive to these parameters above these lower limit values.

Pore size and moisture effects

The porosity of concrete, ϵ, is typically of the order of 0.2. Because the carbonation products, $CaCO_3$ and $3CaCO_3 \cdot 2SiO_2 \cdot 3H_2O$, have higher molar volumes than $Ca(OH)_2(s)$ and $3CaO \cdot 2SiO_2 \cdot 3H_2O$ (CSH), there is a measurable decrease in porosity during carbonation and a concomitant decrease in the average pore radius. Figure 3 shows typical pore-size distributions of noncarbonated and carbonated concrete samples. They were obtained in our laboratory using a combination of nitrogen desorption and mercury porosimetry.

The effect of water is even more important. At any finite relative humidity (RH), a volume fraction of the pores f_K with radii below the corresponding Kelvin radius will be filled with water. The remaining pores will have their walls covered by a H_2O film, the thickness, w in nm, of which can be approximated by (Hagymassy et al., 1969):

$$w = 0.425[-\log(RH/100)]^{-0.31} \quad (15)$$

Consequently a fraction f_w of the total pore volume will be

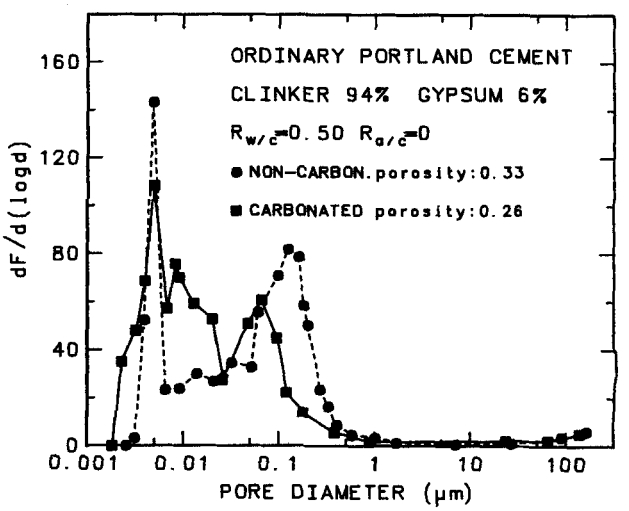

Figure 3. Typical pore-size distribution of completely-hydrated noncarbonated and carbonated concrete samples.

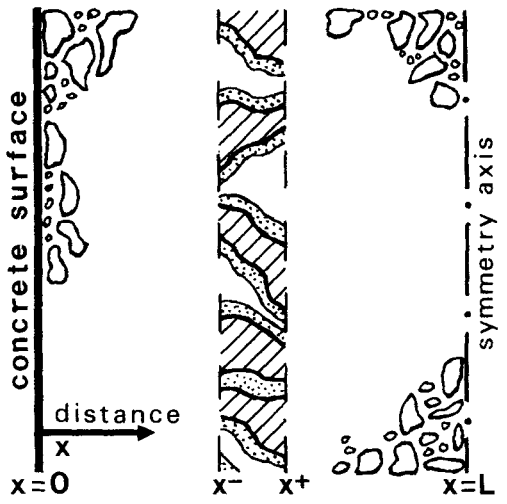

Figure 4. Slab and control volume geometry.

occupied by this aqueous film. If $f = f_K + f_w$ is defined as the total fraction of pore volume filled with water, the rest of the volume, which equals $1 - f$ is available for gaseous CO_2 diffusion. Clearly, this fraction $1 - f$ decreases significantly as ambient humidity increases.

Mathematical Modeling

In order to develop a usable process model of carbonation in a concrete slab of thickness $2L$ (Figure 4) on the basis of the above physical considerations, it is necessary to make certain assumptions. These assumptions are the following:

1. *Initially Macroscopically Uniform Medium.* Of course, any structural changes induced by carbonation, such as change in porosity and surface area, have to be included in the model.

2. *Uniform and Steady Local Humidity.* This implies that, when ϵ is uniform and steady, f_K, f_w, and f are also uniform and steady in time and are in equilibrium with the external relative humidity regardless of the amount of H_2O produced or consumed by the chemical reactions.

On the basis of these assumptions and of the above physical considerations, one can write the following mass balances for gaseous CO_2, solid $Ca(OH)_2$, dissolved $Ca(OH)_2$, calcium silicate hydrate (CSH) and unhydrated silicates (C_3S and C_2S).

Mass Balance of CO_2:

$$\frac{\partial}{\partial t}[\epsilon(1-f)[CO_2]] = \frac{\partial}{\partial x}\left(D_{e,CO_2}\frac{\partial[CO_2]}{\partial x}\right) - \epsilon^0 f_w r_{CH} - 3r_{CSH} - 3r_{C_3S} - 2r_{C_2S} \quad (16)$$

Mass Balance of $Ca(OH)_2$:

$$\frac{\partial}{\partial t}[Ca(OH)_2(s)] = r_{H,CH} - r_D \quad (17)$$

Mass Balance of Dissolved $Ca(OH)_2$:

$$\frac{\partial}{\partial t}[\epsilon f[Ca(OH)_2(aq)]] = \frac{\partial}{\partial x}\left(D_{e,Ca(OH)_2(aq)}\frac{\partial[Ca(OH)_2(aq)]}{\partial x}\right) - \epsilon^0 f_w r_{CH} + r_D \quad (18)$$

Mass Balance of CSH:

$$\frac{\partial}{\partial t}[CSH] = -r_{CSH} + r_{H,CSH} \quad (19)$$

Mass Balances of Unhydrated Silicates:

$$\frac{\partial}{\partial t}[C_3S] = -r_{C_3S} - r_{H,C_3S} \quad (20)$$

$$\frac{\partial}{\partial t}[C_2S] = -r_{C_2S} - r_{H,C_2S} \quad (21)$$

where the rates r defined by Eqs. 1, 2, 3, 6, 8, 9, 12, 13 and 14 are expressed in mol/s · m^3 of concrete.

The corresponding initial and boundary conditions are:

At $t = 0$,

$$\left\{\begin{array}{l}[CO_2] = 0, [Ca(OH)_2(s)] = [Ca(OH)_2(s)]^0 \\ [Ca(OH)_2(aq)] = [Ca(OH)_2(aq)]^0, [CSH] = [CSH]^0 \\ [C_3S] = [C_3S]^0, [C_2S] = [C_2S]^0, \epsilon = \epsilon^0\end{array}\right\} \quad (22)$$

At the surface, $x = 0$,

$$[CO_2] = [CO_2]^0, \qquad \partial[Ca(OH)_2(aq)]/\partial x = 0 \quad (23)$$

Table 2. Change in Concrete Porosity Due to the Hydration and Carbonation Reactions*

Concentration of constituent i at $t_{cu} = 0$

$$[i]_0 = \frac{m_i m_{cl}\rho_c}{MW_i\left(R_{w/c}\frac{\rho_c}{\rho_w} + R_{a/c}\frac{\rho_c}{\rho_a} + 1\right)}$$

Porosity at $t_{cu} = 0$

$$\epsilon_0 = \frac{R_{w/c}\rho_c/\rho_w}{\left(R_{w/c}\frac{\rho_c}{\rho_w} + R_{a/c}\frac{\rho_c}{\rho_a} + 1\right)}$$

Porosity decrease due to hydration

$$\Delta\epsilon_H = \Sigma([i]_0\Delta\bar{V}_i F_i)$$

Porosity decrease due to carbonation**

$$\Delta\epsilon_c = ([Ca(OH)_2(s)]^0 - [Ca(OH)_2(s)])\Delta\bar{V}_{CH} + ([CSH]^0 - [CSH])\Delta\bar{V}_{CSH}$$

Constituent i	C_3S	C_2S	C_3A	C_4AF
$MW_i \times 10^3$ (kg/mol)	228.30	172.22	270.18	485.96
$\Delta\bar{V}_i \times 10^6$ (m^3/mol)	53.28	39.35	149.82	112.81

$\Delta\bar{V}_{CH} = 3.85 \cdot 10^{-6}$ m^3/mol $\Delta\bar{V}_{CSH} = 15.39 \cdot 10^{-6}$ m^3/mol

*Computed with molecular weights and molar volumes of the principal constituents of Portland cement and parameters used in conjunction with Eq. 25.

**The terms involving the unhydrated and subject to carbonation C_3S and C_2S can be omitted because their contribution to porosity change is negligible.

At the symmetry axis, $x = L$,

$$\partial[CO_2]/\partial x = 0, \qquad \partial[Ca(OH)_2(aq)]/\partial x = 0 \qquad (24)$$

It is worth noting again that the initial conditions refer to the end of the curing period.

The local porosity, ϵ, can be computed at any time from the local values of the concentrations of the solid reactants and products from the following equation:

$$\epsilon = \epsilon_0 - \Delta\epsilon_H - \Delta\epsilon_c \qquad (25)$$

where ϵ_0 is the concrete porosity at $t_{cu} = 0$, which depends on the water to cement ratio ($R_{w/c}$) and on the aggregates to cement ratio ($R_{a/c}$). The terms $\Delta\epsilon_H$ and $\Delta\epsilon_c$ account for the change in porosity due to hydration and carbonation, respectively, of cement components. The explicit dependence of ϵ_0, $\Delta\epsilon_H$ and $\Delta\epsilon_c$ on $R_{w/c}$, $R_{a/c}$ and on cement chemical composition is given in Table 2.

Nondimensionalization

The above equations can be written in dimensionless form by introducing the following dimensionless parameters:

$$\left\{\begin{array}{l} C = [CO_2]/[CO_2]^0 \quad C_{CH} = [Ca(OH)_2(s)]/[Ca(OH)_2(s)]^0 \quad C_{CSH} = [CSH]/[CSH]^0 \\ C_{CHL} = [Ca(OH)_2(aq)]/[Ca(OH)_2(aq)]^0 \quad C_{C_3S} = [C_3S]/[C_3S]^0 \quad C_{C_2S} = [C_2S]/[C_2S]^0 \\ z = x/L \quad \Phi^2 = L^2 \dfrac{\epsilon^0 f_w r^0_{CH}}{[CO_2]^0 D^0_{e,CO_2}} \quad \tau = D^0_{e,CO_2} t/[\epsilon^0(1-f)L^2] \quad \psi = \epsilon/\epsilon^0 \quad \varphi = (1-f)/f \\ \delta = D_{e,CO_2}/D^0_{e,CO_2} \quad \delta_{CH} = D^0_{e,Ca(OH)_2(aq)}/D^0_{e,CO_2} \quad \delta_{CHL} = \dfrac{D_{e,Ca(OH)_2(aq)}}{D^0_{e,Ca(OH)_2(aq)}} \end{array}\right\} \qquad (26)$$

$$\left\{\begin{array}{l} \xi_{CH} = r_{CH}/r^0_{CH} \quad \xi_{CSH} = r_{CSH}/r^0_{CSH} \quad \xi_{C_3S} = r_{C_3S}/r^0_{C_3S} \quad \xi_{C_2S} = r_{C_2S}/r^0_{C_2S} \\ \xi_{H,CH} = r_{H,CH}/r^0_{H,CH} \quad \xi_D = r_D/r^0_D \quad \xi_{H,CSH} = r_{H,CSH}/r^0_{H,CSH} \\ \xi_{H,C_3S} = r_{H,C_3S}/r^0_{H,C_3S} \quad \xi_{H,C_2S} = r_{H,C_2S}/r^0_{H,C_2S} \end{array}\right\} \qquad (27)$$

$$\left\{\begin{array}{l} \alpha_{CSH} = r^0_{CSH}/(\epsilon^0 f_w r^0_{CH}) \quad \alpha_{C_3S} = r^0_{C_3S}/(\epsilon^0 f_w r^0_{CH}) \quad \alpha_{C_2S} = r^0_{C_2S}/(\epsilon^0 f_w r^0_{CH}) \\ \alpha_{H,CH} = r^0_{H,CH}/(\epsilon^0 f_w r^0_{CH}) \quad \alpha_D = r^0_D/(\epsilon^0 f_w r^0_{CH}) \quad \alpha_{H,CSH} = r^0_{H,CSH}/(\epsilon^0 f_w r^0_{CH}) \\ \alpha_{H,C_3S} = r^0_{H,C_3S}/(\epsilon^0 f_w r^0_{CH}) \quad \alpha_{H,C_2S} = r^0_{H,C_2S}/(\epsilon^0 f_w r^0_{CH}) \end{array}\right\} \qquad (28)$$

$$\left\{\begin{array}{ll} \beta = \dfrac{[Ca(OH)_2(s)]^0}{\epsilon^0(1-f)[CO_2]^0} & \beta_1 = \dfrac{[Ca(OH)_2(aq)]^0}{[CO_2]^0} \quad \beta_2 = \dfrac{[CSH]^0}{\epsilon^0(1-f)[CO_2]^0} \\ \beta_3 = \dfrac{[C_3S]^0}{\epsilon^0(1-f)[CO_2]^0} & \beta_4 = \dfrac{[C_2S]^0}{\epsilon^0(1-f)[CO_2]^0} \end{array}\right\} \qquad (29)$$

Of the above dimensionless numbers, those defined by Eqs. 27 are dimensionless rates and assume typically values between unity and zero. The parameters defined by Eqs. 28 give a relative measure of the intrinsic rates of the various reactions in comparison to the rate of $CaCO_3$(s) formation, which is intrinsically the second fastest of all reactions involved. The "solid capacity" parameters defined by Eqs. 29 provide a measure of the mass of the material in the concrete medium which can be carbonated, in relation to the ambient CO_2 concentration. Typical values for the α and β parameters defined by Eqs. 28 and 29 are given in Table 3, together with typical values of the diffusivity ratios δ and of the Thiele modulus Φ defined by Eqs. 26. Table 3 provides typical values for the above parameters both for normal exposure, i.e., typical indoor conditions ($p_{CO_2} \approx 5. \cdot 10^{-4}$ bar) and for the conditions of accelerated carbonation tests performed in our laboratory by using a controlled-atmosphere concrete carbonation chamber with $p_{CO_2} = 0.5$ bar. The advantage of this carbonation chamber is that the carbonation process is accelerated dramatically and can be studied experimentally over a time frame of days instead of years, as discussed in the Results section. As shown in Table 3, some of the model parameters remain the same both for the accelerated tests and for normal exposure conditions, but some are seriously affected, as they are inversely proportional to the ambient CO_2 concentration.

On the basis of the above parameters and variables, one can write the model equations (Eqs. 16–21) in the form:

$$\frac{\partial(\psi C)}{\partial\tau} = \frac{\partial}{\partial z}\left(\delta\frac{\partial C}{\partial z}\right) - \Phi^2(\xi_{CH} + 3\alpha_{CSH}\xi_{CSH} + 3\alpha_{C_3S}\xi_{C_3S} + 2\alpha_{C_2S}\xi_{C_2S}) \qquad (30)$$

$$\beta\frac{\partial(C_{CH})}{\partial\tau} = \Phi^2(\alpha_{H,CH}\xi_{H,CH} - \alpha_D\xi_D) \qquad (31)$$

$$(\beta_1/\varphi)\frac{\partial(\psi C_{CHL})}{\partial\tau} = \beta_1\delta_{CH}\frac{\partial}{\partial z}\left(\delta_{CHL}\frac{\partial C_{CHL}}{\partial z}\right) - \Phi^2(\xi_{CH} - \alpha_D\xi_D) \qquad (32)$$

Table 3. Typical Model Parameter Values

Dimensionless Parameters	Normal Exposure 0.05% CO_2	Accelerated Tests 50% CO_2
β	$5.30 \cdot 10^5$	$5.30 \cdot 10^2$
β_1/φ	$3.32 \cdot 10^2$	$3.32 \cdot 10^{-1}$
β_2	$2.97 \cdot 10^5$	$2.97 \cdot 10^2$
β_3	$1.04 \cdot 10^4$	$1.04 \cdot 10^1$
β_4	$5.11 \cdot 10^4$	$5.11 \cdot 10^1$
α_{CSH}	$>1.46 \cdot 10^{-3}$	$>1.46 \cdot 10^{-3}$
α_{C_3S}	$>1.19 \cdot 10^{-3}$	$>1.19 \cdot 10^{-3}$
α_{C_2S}	$>1.41 \cdot 10^{-3}$	$>1.41 \cdot 10^{-3}$
α_D	$8.70 \cdot 10^3$	8.70
$\alpha_{H,CH}$	$1.58 \cdot 10^{-4}$	$1.58 \cdot 10^{-7}$
$\alpha_{H,CSH}$	$1.11 \cdot 10^{-4}$	$1.11 \cdot 10^{-7}$
α_{H,C_3S}	$4.63 \cdot 10^{-5}$	$4.63 \cdot 10^{-8}$
α_{H,C_2S}	$1.77 \cdot 10^{-4}$	$1.77 \cdot 10^{-7}$
φ	3.16	3.16
δ_{CH}	$5.52 \cdot 10^{-5}$	$5.52 \cdot 10^{-5}$
Φ	405	405

$$\beta_2 \frac{\partial(C_{CSH})}{\partial \tau} = -\Phi^2(\alpha_{CSH}\xi_{CSH} - \alpha_{H,CSH}\xi_{H,CSH}) \quad (33)$$

$$\beta_3 \frac{\partial(C_{C_3S})}{\partial \tau} = -\Phi^2(\alpha_{C_3S}\xi_{C_3S} + \alpha_{H,C_3S}\xi_{H,C_3S}) \quad (34)$$

$$\beta_4 \frac{\partial(C_{C_2S})}{\partial \tau} = -\Phi^2(\alpha_{C_2S}\xi_{C_2S} + \alpha_{H,C_2S}\xi_{H,C_2S}) \quad (35)$$

with initial and boundary conditions:

At $\tau = 0$,

$$C = 0, \quad C_{CH} = C_{CHL} = C_{CSH} = C_{C_3S} = C_{C_2S} = 1 \quad (36)$$

$$\text{At} \quad z = 0, \quad C = 1, \quad \partial C_{CHL}/\partial z = 0 \quad (37)$$

$$\text{At} \quad z = 1, \quad \partial C/\partial z = 0, \quad \partial C_{CHL}/\partial z = 0 \quad (38)$$

It should be noted that, once Eqs. 30–35 have been solved with the initial and boundary conditions Eqs. 36–38, the pH at each point in space and time can be computed from:

$$pH = pK_w + \log(2. \cdot 10^{-3}[\text{Ca(OH)}_2(\text{aq})]^0 C_{CHL}) \quad (39)$$

Inspection of Eqs. 30–35 in conjunction with Table 3, which lists typical values of the dimensionless parameters, reveals the following:

a) The values of the "solid capacity" terms, β, β_2, β_3, and β_4, are of the order of 10^4–10^5 for normal exposure conditions and of the order of 10–500 for the accelerated test conditions. Consequently, the solid concentration time derivatives are much smaller than $\partial(\psi C)/\partial\tau$ and therefore the pseudosteady-state approximation (Wen, 1968) can be safely applied for gaseous CO_2, both for normal exposure and for accelerated test conditions: i.e., Eq. 30 can be replaced by

$$\frac{d}{dz}\left(\delta \frac{dC}{dz}\right) = \Phi^2(\xi_{CH} + 3\alpha_{CSH}\xi_{CSH} + 3\alpha_{C_3S}\xi_{C_3S} + 2\alpha_{C_2S}\xi_{C_2S}) \quad (40)$$

Table 4. Carbonation Rates of $Ca(OH)_2$ and Cement Components and Dissolution Rate of $Ca(OH)_2$(s)

Reaction	Dimensional Form	Dimensionless Form
8	$r_D = (1/2)\epsilon f_w k_{s,CH}([OH^-]_{eq} - [OH^-])$	$\xi_D = 1 - C_{CHL}$
9	$r_{CH} = HRTk_2[OH^-]\,[CO_2]$	$\xi_{CH} = C_{CHL}C$
12	$r_{CSH} = k_{CSH}a_{s,CSH}\,[CO_2]$	$\xi_{CSH} = C_{CSH}C$
13	$r_{C_3S} = k_{C_3S}a_{s,C_3S}\,[CO_2]$	$\xi_{C_3S} = C_{C_3S}C$
14	$r_{C_2S} = k_{C_2S}a_{s,C_2S}\,[CO_2]$	$\xi_{C_2S} = C_{C_2S}C$

b) The $Ca(OH)_2$(aq) diffusion term in Eq. 32 can be neglected in good approximation even for the normal exposure conditions. In this case, the β_1/φ "liquid capacity" term is of the order of 300. Also $\beta_1\delta_{CH}$ varies between 10^{-5} and 10^{-2}, while Φ^2 is of the order of 10^5. It follows then that $\xi_{CH} \approx \alpha_D\xi_D$ and therefore $C_{CHL} \approx C_{CH}$ everywhere in the concrete volume. Therefore, Eq. 32 can, in good approximation, be replaced by:

$$C_{CHL} = C_{CH} \quad (41)$$

c) Since Φ^2 is of the order of 10^5, it follows from Eq. 30 or 40 that the value of ξ_{CH} must be of the order of 10^{-6}, which implies, in view of Eq. 9 and Table 4, that either C or C_{CHL} must vanish, i.e., $C \cdot C_{CHL} \approx 0$ everywhere in the concrete volume. This implies that a *reaction front* between CO_2(g) and $Ca(OH)_2$ (aq) exists at some normalized distance z_c from the concrete surface (Figure 5), i.e.:

$$C_{CHL} = 0 \quad \text{and} \quad d^2C/dz^2 = 0 \quad \text{for} \quad 0 \le z < z_c \quad (42a)$$

$$C = 0 \quad \text{for} \quad z_c < z \le 1 \quad (42b)$$

In view of observation a, it also follows that $C_{CH} = 0$ for $0 \le z \le z_c$. Similarly, one can use Eq. 40 and Table 3 to show that, because of the magnitudes of the Φ^2, α_{CSH}, α_{C_3S} and α_{C_2S} terms, the ξ_{CSH}, ξ_{C_3S} and ξ_{C_2S} terms must also vanish everywhere

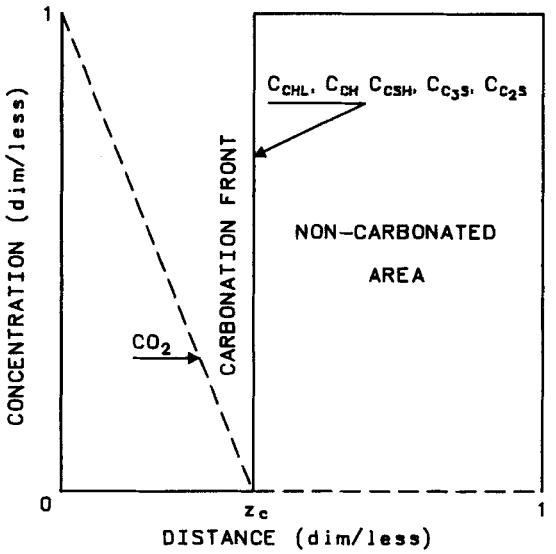

Figure 5. Typical concentration profiles during concrete carbonation.

in the concrete volume. Therefore, the concentrations C_{CSH}, C_{C_3S} and C_{C_2S} must also vanish between the reaction front and the concrete surface, i.e.:

$$C_{CSH} = C_{C_3S} = C_{C_2S} = 0 \quad \text{for} \quad 0 \le z < z_c \tag{42c}$$

It follows from Eq. 42a and from the boundary conditions 37 and 38 that the gaseous CO_2 concentration profile inside the carbonated zone, i.e., for $0 \le z \le z_c$, is given by:

$$C = 1 - z/z_c; \; 0 \le z \le z_c \tag{42d}$$

The remaining problem is to determine the location of the carbonation front z_c as a function of time.

Model solution

According to the above discussion, the model equations can be written, in good approximation, in the following simplified form:

$$\frac{d}{dz}\left(\delta \frac{dC}{dz}\right) = \Phi^2(\xi_{CH} + 3\alpha_{CSH}\xi_{CSH} + 3\alpha_{C_3S}\xi_{C_3S} + 2\alpha_{C_2S}\xi_{C_2S}) \tag{43a}$$

$$\beta\frac{\partial(C_{CH})}{\partial\tau} = \Phi^2(\alpha_{H,CH}\xi_{H,CH} - \xi_{CH}) \tag{43b}$$

$$C_{CHL} = C_{CH} \tag{43c}$$

$$\beta_2 \frac{\partial(C_{CSH})}{\partial\tau} = -\Phi^2(\alpha_{CSH}\xi_{CSH} - \alpha_{H,CSH}\xi_{H,CSH}) \tag{43d}$$

$$\beta_3 \frac{\partial(C_{C_3S})}{\partial\tau} = -\Phi^2(\alpha_{C_3S}\xi_{C_3S} + \alpha_{H,C_3S}\xi_{H,C_3S}) \tag{43e}$$

$$\beta_4 \frac{\partial(C_2S)}{\partial\tau} = -\Phi^2(\alpha_{C_2S}\xi_{C_2S} + \alpha_{H,C_2S}\xi_{H,C_2S}) \tag{43f}$$

Taking into account the relations between the hydration reaction terms, i.e., Eqs. 3 and 6, one can combine Eqs. 43a to 43f in the form:

$$\beta \frac{\partial(C_{CH})}{\partial\tau} + 3\beta_2 \frac{\partial(C_{CSH})}{\partial\tau} + 3\beta_3 \frac{\partial(C_{C_3S})}{\partial\tau} + 2\beta_4 \frac{\partial(C_{C_2S})}{\partial\tau} = -\frac{d}{dz}\left(\delta \frac{dC}{\partial z}\right) \tag{44}$$

Also according to the previous discussion, the following Equations hold:

$$\left.\begin{aligned} &C = 1 - z/z_c \\ &C_{CHL} = C_{CH} = C_{CSH} = C_{C_3S} = C_{C_2S} = 0 \end{aligned}\right\} \quad \text{for} \quad 0 \le z < z_c \tag{45a}$$

$$\left.\begin{aligned} &C = 0 \\ &C_{CHL} = C_{CH} = C_{CSH} = C_{C_3S} = C_{C_2S} = 1 \end{aligned}\right\} \quad \text{for} \quad z_c < z \le 1 \tag{45b}$$

Using Eqs. 44 and 45, one can determine the dependence of the carbonation front location z_c on time τ:

$$\frac{dz_c}{d\tau} = \frac{\left(\delta \frac{dC}{dz}\right)_{z_c^+} - \left(\delta \frac{dC}{dz}\right)_{z_c^-}}{(\beta C_{CH} + 3\beta_2 C_{CSH} + 3\beta_3 C_{C_3S} + 2\beta_4 C_{C_2S})_{\tau(z_c+)} - (\beta C_{CH} + 3\beta_2 C_{CSH} + 3\beta_3 C_{C_3S} + 2\beta_4 C_{C_2S})_{\tau(z_c-)}} \tag{46a}$$

i.e.,

$$\frac{dz_c}{d\tau} = \frac{\delta_c}{(\beta + 3\beta_2 + 3\beta_3 + 2\beta_4)z_c} \tag{46b}$$

where δ_c denotes the value of $\delta = D_{e,CO_2}/D^0_{e,CO_2}$ within the totally carbonated volume $0 \le z \le z_c$. Solution of Eq. 46b with initial condition $z_c = 0$ at $\tau = 0$ gives:

$$z_c = \sqrt{\frac{2\delta_c\tau}{\beta + 3\beta_2 + 3\beta_3 + 2\beta_4}} \tag{47a}$$

or, equivalently, in dimensional form:

$$x_c = \sqrt{\frac{2[CO_2]^0 D_{e,CO_2,c}t}{[Ca(OH)_2(s)]^0 + 3[CSH]^0 + 3[C_3S]^0 + 2[C_2S]^0}} \tag{47b}$$

In completely hydrated concrete $[C_3S]^0$ and $[C_{C_2S}]^0$ equal zero and Eqs. 47 become:

$$z_c = \sqrt{\frac{2\delta_c\tau}{\beta + 3\beta_2}} \tag{48a}$$

$$x_c = \sqrt{\frac{2[CO_2]^0 D_{e,CO_2,c}t}{[Ca(OH)_2(s)]^0 + 3[CSH]^0}} \tag{48b}$$

Equations 47 and 48 provide, for the first time, a theoretical basis for predicting the proportionality constant A in the empirical expression:

$$x_c = A\sqrt{t} \tag{49}$$

which has been reported in the literature to describe the carbonation front location dependence on time (Hamada, 1969; Alekseev and Rozental, 1969; Meyer, 1969; Alexandre, 1976). As shown below, Eqs. 47 and 48 agree well with experimental results obtained both under normal exposure and under accelerated test conditions. In the former case, the "liquid capacity" term (β_1/φ) may be significant and should be added to the solid capacity terms in the denominator of Eqs. 47a and 48a. However, this need not be done if the $[Ca(OH)_2(s)]^0$ concentration term in β refers to the total concentration of $Ca(OH)_2$ in the concrete volume.

Effective diffusivity of CO_2 in carbonated concrete

Equations 47 and 48 show that the velocity of the carbonation front depends crucially on the effective diffusivity of CO_2 in the pores of carbonated concrete. Although the value of this param-

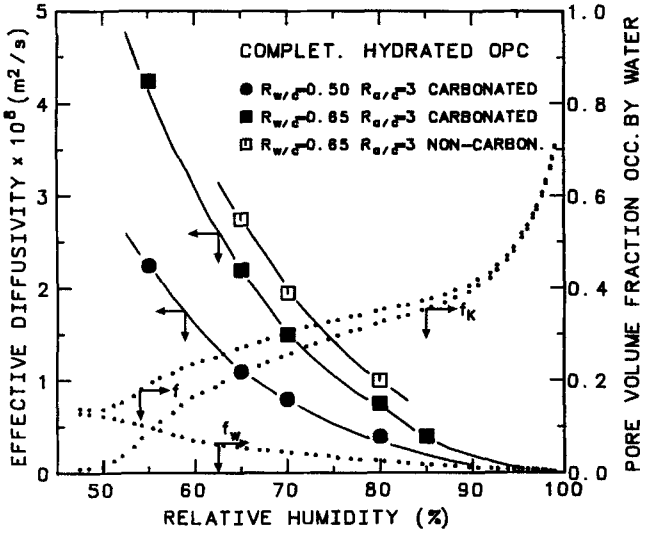

Figure 6. Effect of relative humidity of ambient air on the effective diffusivity of CO_2 and volume fractions f_K, f_w and f of pores occupied by water.

eter can be estimated by means of standard models once the pore size distribution of concrete has been measured and the ambient relative humidity value has been specified, it was decided to directly measure D_{e,CO_2} using an apparatus of the Wicke-Kallenbach type. Details of this experimental investigation will be given in a future publication.

The experimentally determined D_{e,CO_2} values are in reasonable agreement with standard models. For example, the experimental results can be fitted within the parallel pore model with tortuosity values of the order of 3 or within the Wakao-Smith micropore-macropore model within a factor of 50%. As expected, D_{e,CO_2}, which is typically of the order of 10^{-8} m^2/s, was found to depend strongly on the water to cement ratio of the concrete samples. The effect of aggregates was also investigated and modeled and results will be presented in a separate paper.

Figure 6 shows the effect of ambient relative humidity on D_{e,CO_2} for a completely hydrated concrete sample before and after carbonation. Computed values of f_K, f_w and f based on the measured pore-size distribution of the sample are also shown on the figure. The value of D_{e,CO_2} decreases dramatically with increasing ambient relative humidity and with f.

Comparison of Theory and Experiment

Previous experimental studies of concrete carbonation (Tuutti, 1982; Nagataki et al., 1986; Ying-yu and Qui-dong, 1987; Nagataki et al., 1988) have established that the location of the carbonation front proceeds proportionally with $\sqrt{t}$, i.e.:

$$x_c = A\sqrt{t} \tag{49}$$

There is almost unanimous agreement among previous workers about this functional dependence, at least when the experiments have been conducted under controlled indoor conditions (Hamada, 1969; Schiessl, 1976; Nagataki et al., 1988; Richardson, 1988). For outdoor conditions, some deviations from Eq. 49 have been reported (Schiessl, 1976; Nagataki et al., 1986). This is to be expected, since, according to the present theoretical analysis, significant variations in relative ambient humidity will affect D_{e,CO_2} and will result in significant variation of the proportionality constant A as a function of time. A practical problem faced by most previous workers was the very long time needed to perform the experiments under normal exposure conditions (i.e., $p_{CO_2} \approx 0.0005$ bar). Typically 5–10 years are required, whereas, in some cases, samples were studied for as long as 20 years (Nagataki et al., 1986; Litvan and Meyer, 1986).

In order to overcome this problem, we have constructed an accelerated test apparatus, in which unhydrated or hydrated concrete samples are exposed to $p_{CO_2} \approx 0.5$ bar at constant temperature and relative humidity.

In view of Eqs. 47 and 48, this leads to a dramatic reduction in the experimental time needed to perform the experiments. Thus to achieve the same carbonation depth, e.g., 1 cm, the ratio t_1/t_2 ($= p_{CO_2,2}/p_{CO_2,1}$) of the time t_1 required under normal exposure conditions and of the time t_2 required under accelerated test conditions, is 1,000. Therefore, one can study in the laboratory within a few days what would happen under normal exposure conditions within many years. It is important to note that the same front location equations (Eqs. 47 and 48) are valid both for normal exposure and for accelerated test conditions. This is because the values of the dimensionless parameters (Table 3) which govern the process of carbonation are such that the same simplifications which lead from the general equations (Eqs. 30–35) to the simplified equations (Eqs. 43) are valid both for the normal exposure and for the accelerated test conditions. This has been also verified by numerical solution of Eqs. 30–35, using the finite difference method. It was found that the results are practically identical with those predicted by Eqs. 47 and 48 for relative humidities above 40%. For smaller values of relative humidity, there are significant deviations, since the Φ^2 term decreases substantially and, consequently, no sharp front is formed under these conditions. However, ambient relative humidities less than 40–50% are rarely found in practice.

Figure 7a shows typical experimental x_c *vs.* $\sqrt{t}$ results obtained in the accelerated test apparatus. The solid lines correspond to Eq. 48 with D_{e,CO_2} measured *independently* in the Wicke-Kallenbach apparatus. It can be seen that the agreement between theory and experiment is excellent. As expected, Figure 7a also shows that an increase in the water to cement ratio ($R_{w/c}$) of the concrete, which increases concrete porosity, also increases the velocity of propagation of the carbonation front.

Figures 7b and 7c show the experimental results of Ying-yu and Qui-dong (1987) and Nagataki et al. (1988) who are the only previous workers known to the authors who have published results of accelerated test experiments with specified $R_{w/c}$, $R_{a/c}$ and relative humidity conditions. The solid lines on the figures again correspond to Eq. 48 with D_{e,CO_2} measured in our laboratory for the experimental conditions of these investigations, i.e., 52% and 60% relative humidity, respectively, and $R_{w/c} = 0.4, 0.5$ and 0.6, respectively. Again, agreement between theory and experiment is excellent.

As shown on Figure 8, Eq. 48 can also describe very well experimental results obtained under indoor normal exposure conditions, i.e., over a period of several years. The solid lines on the figure correspond again, via Eq. 48, to D_{e,CO_2} values measured in our laboratory for the $R_{w/c}$ and relative humidity conditions of Nagataki et al. (1986).

In general, Eq. 48 is in excellent agreement with experiment, both for accelerated test and for normal exposure conditions,

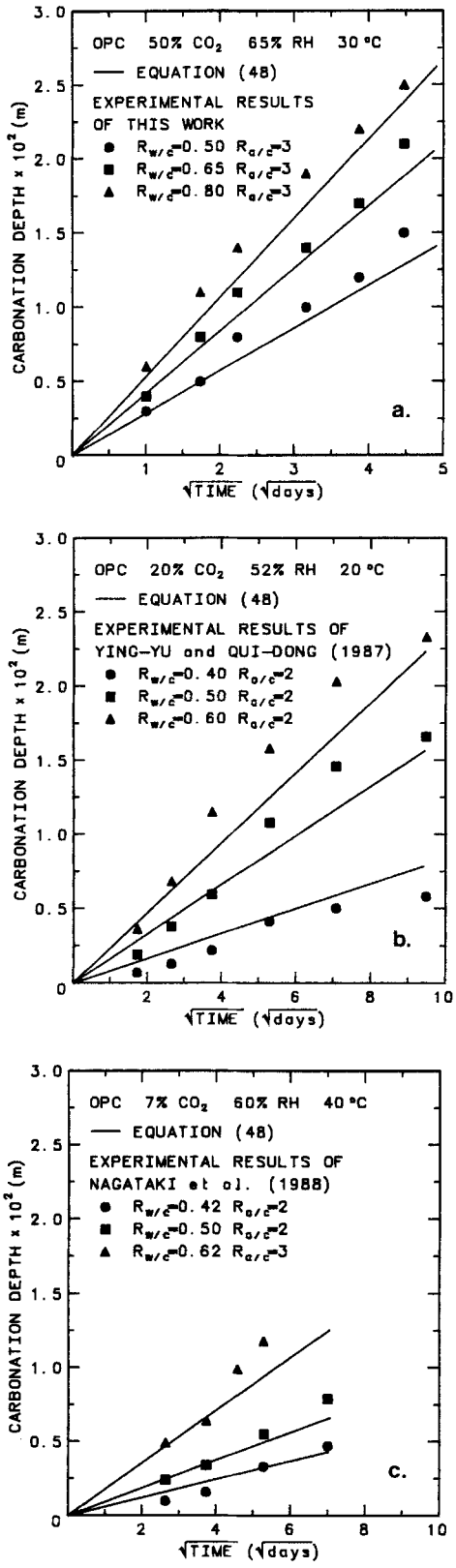

Figure 7. Effect of time on carbonation depth under accelerated test conditions for $R_{w/c}$ ratios and comparison with theory.

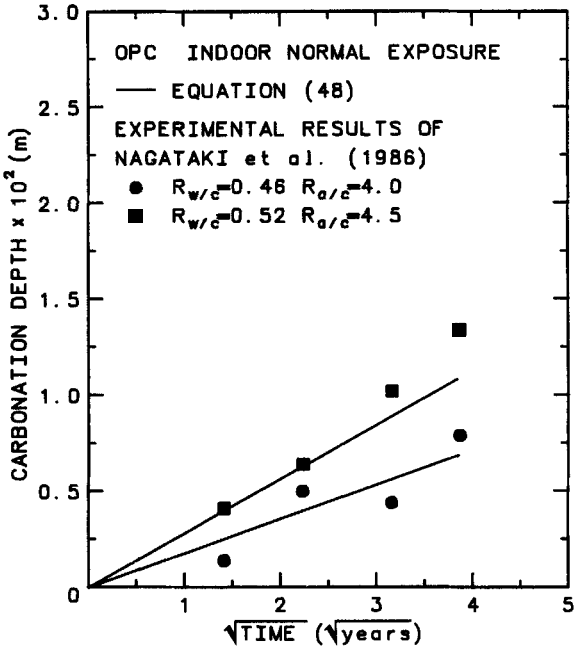

Figure 8. Effect of time on carbonation depth under indoor normal exposure conditions and comparison with theory.

despite the fact that the time scales of the experiments differ by three orders of magnitude for these two conditions.

Effect of relative humidity

Increasing ambient relative humidity increases the fraction f of the pores filled with water and thus hinders diffusion of CO_2. Consequently, the velocity of the carbonation front decreases. This is shown on Figure 9, where experimental results obtained in the accelerated test apparatus are compared with the solid line which corresponds to Eq. 48. Agreement is excellent for rel-

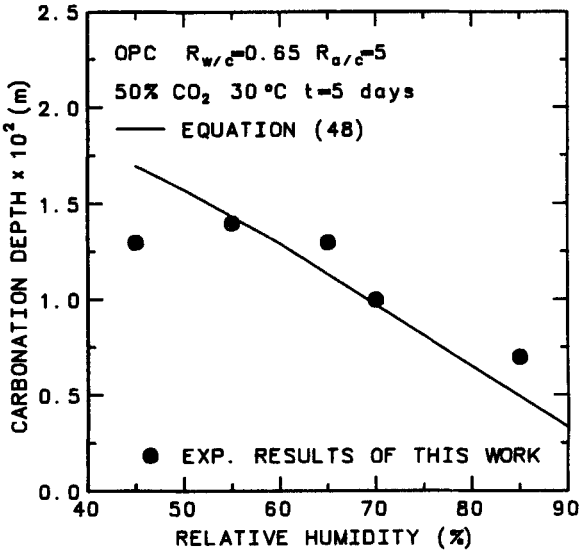

Figure 9. Effect of relative humidity on the depth of carbonation.

ative humidities above 50%. Figure 9 provides experimental and theoretical support to the empirical observation that the carbonation of concrete is more serious a problem in dry climates or under conditions sheltered from rain (e.g., indoor conditions). If relative humidities are reduced to values below 50% Eq. 48 predicts that there should be a continuing increase in the velocity of the carbonation front, since D_{e,CO_2} is increasing. However, as shown on Figure 9, the experiments show that the front velocity is decreasing, in good qualitative agreement with the empirical observation that the speed of carbonation goes through a maximum at an ambient humidity of about 50–65%. The reason for the disagreement between experiment and Eq. 48 at relative humidities below 50% simply is that the model simplifications leading to Eq. 48 are not valid in this region. This is because the decrease in f in this region causes a decrease in the Thiele modulus Φ of the carbonation reaction and, consequently, no sharp carbonation front is formed. In this region, diffusion of CO_2 ceases to be the rate-limiting step of the carbonation process and the chemical kinetics of the carbonation reaction become important. One then needs to solve numerically the complete set of Eqs. 30 to 35 in order to determine the time evolution of the pH value in the concrete volume. Experimental and theoretical results in this region of very low ambient relative humidities will be discussed in a future publication. Equations 47 and 48, however, describe successfully the carbonation process over the vast majority of usual ambient environmental conditions.

Conclusions

A mathematical model based on fundamental reaction engineering principles has been developed to describe the process of concrete carbonation, which is a major time-limiting factor for the durability of reinforced concrete. The model shows that this apparently complex physicochemical process can, in most practical cases, be described by a simple equation which is in excellent agreement with experiment.

Acknowledgment

Financial support by the Hellenic Secretariat of Research and Technology is gratefully acknowledged. We also thank Dr. E. Galanoulis of the TITAN cement company for helpful discussions and our reviewers for their thoughtful and constructive suggestions.

Notation

$a_{s,j}$ = liquid exposed surface area of constituent j, m^2/m^3
A = proportionality constant of empirical square-root law, $m/s^{1/2}$
C = dimensionless concentration of CO_2
$[C_2S]$ = molar concentration of C_2S, mol/m_t^3
$[C_3S]$ = molar concentration of C_3S, mol/m_t^3
C_{C_2S} = dimensionless concentration of C_2S
C_{C_3S} = dimensionless concentration of C_3S
C_{CH} = dimensionless concentration of $Ca(OH)_2(s)$
C_{CHL} = dimensionless concentration of $Ca(OH)_2(aq)$
C_{CSH} = dimensionless concentration of CSH
$[Ca(OH)_2(aq)]$ = molar concentration of $Ca(OH)_2(aq)$ in the liquid phase, mol/m_l^3
$[Ca(OH)_2(s)]$ = molar concentration of $Ca(OH)_2(s)$, mol/m_t^3
$[CO_2]$ = molar concentration of CO_2 in the gas phase, mol/m_g^3
[CSH] = molar concentration of CSH, mol/m_t^3
d = pore diameter, μm
$D_{e,Ca(OH)_2(aq)}$ = effective diffusivity of $Ca(OH)_2(aq)$ in the liquid phase, $m_l^3/m_t \cdot s$
D_{e,CO_2} = effective diffusivity of CO_2, $m_g^3/m_t \cdot s$
f = total fraction of pore volume filled with water, m_l^3/m_{l+g}^3
f_K = volume fraction of pores with radii below the Kelvin radius, m_l^3/m_{l+g}^3
f_w = volume fraction of pores occupied by the aqueous film, m_l^3/m_{l+g}^3
F = porosity fraction of the pores with diameters below d, %
F_i = hydrated fraction of constituent i
H = solubility coefficient in Henry's law, $mol/m^3 \cdot bar$
k_2 = rate constant for the reaction between CO_2 and OH^- ions, $m^3/mol \cdot s$
$k_{H,i}$ = rate constant of hydration of constituent i, s^{-1}
k_j = rate constant for the reaction between constituent j and CO_2, m/s
k_s = mass transfer coefficient for the dissolution of $Ca(OH)_2(s)$, m/s
K_W = equilibrium constant of self-ionization of water
L = distance between outer surface of concrete and axis of symmetry, m
m_{cl} = weight fraction of clinker in cement
m_i = weight fraction of constituent i in clinker
MW_i = molecular weight of constituent i
n_i = hydration power-law coefficient of constituent i
$[OH^-]$ = molar concentration of OH^- ions in the liquid phase, mol/m_l^3
$[OH^-]_{eq}$ = saturation concentration of OH^- ions in the liquid phase, mol/m_l^3
p_{CO_2} = partial pressure of CO_2 in the gas phase, bar
r_D = rate of dissolution of $Ca(OH)_2(s)$ in pore water per unit total volume, $mol/m_t^3 \cdot s$
$r_{H,CH}$ = rate of $Ca(OH)_2$ formation due to the hydration reactions, $mol/m_t^3 \cdot s$
$r_{H,CSH}$ = rate of CSH formation due to the hydration reactions, $mol/m_t^3 \cdot s$
$r_{H,i}$ = rate of constituent i consumption by hydration, $mol/m_t^3 \cdot s$
r_j = rate of constituent j reaction with CO_2 per unit total volume, $mol/m_t^3 \cdot s$
R = gas constant
$R_{a/c}$ = aggregate to cement ratio by weight
$R_{w/c}$ = water to cement ratio by weight
RH = relative humidity of gas phase, %
t = time since the beginning of carbonation, s
t_{cu} = time of curing of concrete, before the beginning of carbonation, s
T = absolute temperature, K
w = thickness of water film in the pores, nm
x = distance from the outer surface of concrete, m
x_c = carbonation depth, m
z = dimensionless distance
z_c = dimensionless carbonation depth

Greek letters

α_D = dimensionless ratio of maximum dissolution rate of $Ca(OH)_2(aq)$ to maximum carbonation rate of $Ca(OH)_2(aq)$
$\alpha_{H,i}$ = dimensionless ratio of maximum hydration rate of constituent i to maximum carbonation rate of $Ca(OH)_2(aq)$
α_j = dimensionless ratio of maximum carbonation rate of constituent j to maximum carbonation rate of $Ca(OH)_2(aq)$
β = dimensionless ratio of $Ca(OH)_2(s)$ concentration in the concrete to the ambient CO_2 concentration
β_1 = dimensionless ratio of $Ca(OH)_2(aq)$ concentration in the concrete to the ambient CO_2 concentration
β_2 = dimensionless ratio of CSH concentration in the concrete to the ambient CO_2 concentration
β_3 = dimensionless ratio of C_3S concentration in the concrete to the ambient CO_2 concentration
β_4 = dimensionless ratio of C_2S concentration in the concrete to the ambient CO_2 concentration
δ = dimensionless effective diffusivity of CO_2

δ_{CH} = dimensionless ratio of maximum effective diffusivity of $Ca(OH)_2$(aq) to maximum effective diffusivity of CO_2

δ_{CHL} = dimensionless effective diffusivity of $Ca(OH)_2$(aq)

$\Delta\bar{V}_{CH}$ = molar volume changes due to the carbonation of $Ca(OH)_2$(s), m^3/mol

$\Delta\bar{V}_{CSH}$ = molar volume changes due to the carbonation of CSH, m^3/mol

$\Delta\bar{V}_i$ = molar volume changes due to the hydration of constituent i, m^3/mol

$\Delta\epsilon_c$ = porosity change due to the carbonation, defined in Table 2

$\Delta\epsilon_H$ = porosity change due to the hydration, defined in Table 2

ϵ = concrete porosity, m^3_{g+l}/m^3_t

ϵ^0 = concrete porosity at $t = 0$

ϵ_0 = porosity at $t_{cu} = 0$

ξ_D = dimensionless rate of dissolution of $Ca(OH)_2$(s)

$\xi_{H,j}$ = dimensionless rate of hydration of constituent j

ξ_j = dimensionless rate of carbonation of constituent j

ρ_a = density of aggregates, kg/m^3

ρ_c = density of cement, kg/m^3

ρ_w = density of water, kg/m^3

τ = dimensionless time, defined in Eq. 26

φ = gas phase volume to liquid phase volume ratio, m^3_g/m^3_l

Φ = Thiele modulus, defined in Eq. 26

ψ = dimensionless porosity, defined in Eq. 26

Subscripts

0 = quantities referring to $t_{cu} = 0$

c = quantities referring to carbonated area

g = quantities referring to the gas phase in the pores

i = constituent of cement, i.e., C_3S, C_2S, C_3A, C_4AF

j = constituent of cement subject to carbonation, i.e., $Ca(OH)_2$(s), CSH, C_3S, C_2S

l = quantities referring to liquid phase of pores

$\bar{S}$ = quantity values in the presence of gypsum

t = quantities referring to total volume of concrete

Superscript

0 = quantities referring to initial conditions ($t = 0$); for the rates value corresponding to initial reactant concentrations

Literature Cited

Alekseev, S. N., and N. K. Rozental, "Kinetika Karbonizatsii Betona," *Beton i Zhelezobeton*, **4**, 22(1969).

Alexandre, J., "Vitesse de Carbonatation," *Proc. RILEM Inter. Symp. on the Carbon. of Concr.*, 6 (1976).

Baird, T., A. G. Cairns-Smith, and D. S. Snell, "Morphology and CO_2 Uptake in Tobermorite Gel," *J. Colloid and Interf. Sci.*, **50**(2), 387 (1975).

Bensted, J., "Hydration of Portland Cement," *Advances in Cement Technology*, S. N. Ghosh, ed., Pergamon Press, New York (1983).

Brunauer, S., and L. E. Copeland, "The Chemistry of Concrete," *Scientific Amer.* **210**(4), 80 (1964).

Danckwerts, P. V., *Gas-Liquid Reactions*, McGraw-Hill, New York (1970).

Frigione, G., "Gypsum in Cement," *Advances in Cement Technology*, S. N. Ghosh, ed., Pergamon Press, New York (1983).

Goodbrake, C. J., J. F. Young, and R. L. Berger, "Reaction of Beta-Dicalcium Silicate and Tricalcium Silicate with Carbon Dioxide and Water Vapor," *J. Amer. Ceram. Soc.*, **62**(3–4), 168(1979).

Hagymassy, Jr., J., S. Brunauer, and R. Sh. Mikhail, "Pore Structure Analysis by Water Vapor Adsorption. I: t-Curves for Water Vapor," *J. Colloid and Interf. Sci.*, **29**(3), 485 (1969).

Hamada, M., "Neutralization (Carbonation) of Concrete and Corrosion of Reinforcing Steel," *Proc. Int. Symp. on the Chem. of Cem.*, **3**, 343 (1969).

Litvan, G. G., and A. Meyer, "Carbonation of Granulated Blast Furnace Slag Cement Concrete During Twenty Years of Field Exposure," *Proc. Int. Conf. on the Use of Fly Ash, Silica Fume, Slag and Natural Pozzolans in Concrete*, ACI SP 91-71, 1445 (1986).

Meyer, A., "Investigations on the Carbonation of Concrete," *Proc. Int. Symp. on the Chem. of Cem.*, **3**, 394 (1969).

Nagataki, S., H. Ohga, and E. K. Kim, "Effect of Curing Conditions on the Carbonation of Concrete with Fly Ash and the Corrosion of Reinforcement in Long-Term Tests," *Proc. Int. Conf. on the Use of Fly Ash, Silica Fume, Slag and Natural Pozzolans in Concrete*, ACI SP 91-24, 521(1986).

Nagataki, S., M. A. Mansur, and H. Ohga, "Carbonation of Mortar in Relation to Ferrocement Construction," *ACI Mat. J.*, **85**(1), 17(1988).

Pereira, C. J., and L. L. Hegedus, "Diffusion and Reaction of Chloride Ions in Porous Concrete," *Proc. Int. Symp. on Chem. Reaction Eng.*, Edimburgh (1984).

Ramachandran, P. A., and M. M. Sharma, "Adsorption with Fast Reaction in a Slurry Containing Sparingly Soluble Fine Particles," *Chem. Eng. Sci.*, **24**, 1681(1969).

Richardson, M. G., *Carbonation of Reinforced Concrete*, Citis Ltd., Dublin (1988).

Sauman, Z., "Carbonization of Porous Concrete and its Main Binding Components," *Cem. Concr. Res.*, **1**, 645(1971).

Schiessl, P., "Zur Frage der Zulässigen Rissbreite und der Erforderlichen Betondeckung im Stahlbetonbau unter Besonderer Berücksichtigung der Karbonatisierung des Betons," *Deutscher Ausschuss für Stahlbeton*, **255** (1976).

Suzuki, K., T. Nishikawa, and S. Ito, "Formation and Carbonation of C-S-H in Water," *Cem. Concr. Res.*, **15**(2), 213 (1985).

Taylor, H. F. W., "Chemistry of Cement Hydration," *Proc. Int. Cong. on the Chem. of Cement*, **1**, 82 (1986).

Tuutti, K., *Corrosion of Steel in Concrete*, CBI Forskning Research, Swedish Cement and Concrete Research Institute, Stockholm (1982).

Wen, C. Y., "Noncatalytic Heterogeneous Solid Fluid Reaction Models," *Ind. Eng. Chem.*, **60**(9), 34 (1968).

Ying-yu, L., and W. Qui-dong, "The Mechanism of Carbonation of Mortar and the Dependence of Carbonation on Pore Structure," *Proc. Katharine and Bryant Mather Int. Conf. on Concr. Durability*, ACI SP 100-98, 1915 (1987).

Manuscript received Apr. 24, 1989, and revision received July 11, 1989.